Reports

High-Pressure Chemistry of Hydrogen in Metals: In Situ Study of Iron Hydride

J. V. Badding, R. J. Hemley, H. K. Mao

Optical observations and x-ray diffraction measurements of the reaction between iron and hydrogen at high pressure to form iron hydride are described. The reaction is associated with a sudden pressure-induced expansion at 3.5 gigapascals of iron samples immersed in fluid hydrogen. Synchrotron x-ray diffraction measurements carried out to 62 gigapascals demonstrate that iron hydride has a double hexagonal close-packed structure, a cell volume up to 17% larger than pure iron, and a stoichiometry close to FeH. These results greatly extend the pressure range over which the technologically important iron-hydrogen phase diagram has been characterized and have implications for problems ranging from hydrogen degradation and embrittlement of ferrous metals to the presence of hydrogen in Earth's metallic core.

THE BEHAVIOR OF HYDROGEN IN metallic environments governs the physical properties of a wide range of materials of fundamental, technological, and planetary interest. These include pure metallic hydrogen, which is formed at ultrahigh pressures and is a subject of intense experimental study (*1*), and metallic hydrides, which are formed in chemical reactions between metals and hydrogen (*2*). Because of the similarities in their dynamical behavior, metal hydrides may share with metallic hydrogen unusual physical properties (*3, 4*). Iron hydride, in particular, is important to the technological problem of hydrogen degradation of ferrous metals (*5*), and is of geologic interest, because of the high cosmic abundances of iron and hydrogen (*6*). Like the transition elements to the right of manganese in the periodic table, iron hydride cannot be synthesized by direct reaction with hydrogen at ambient pressure (*7*). Evidence for its formation has been obtained from experiments carried out at high pressures and temperatures (*8, 9*). However, detailed information about the iron-hydrogen reaction and the physical properties of iron hydride is limited because the reaction must be performed at high pressures and the compound is unstable at ambient conditions.

Because of recent advances in high-pressure diamond cell technology (*10*), it is now possible to study the physical properties of materials at very high pressures, including measurements in the 300 gigapascal (GPa) range (*1, 11*). Here we present the direct observation of the iron-hydrogen reaction by detailed study with a diamond cell. With new synchrotron diffraction techniques, we have determined in situ the crystal structure and equation of state of iron hydride to 62 GPa. The high-pressure stability of this material has implications for understanding hydrogen uptake in metals, including hydrogen storage (*12*) and embrittlement (*5*), and the containment of hydrogen in high-pressure devices (*1*). These results also provide constraints on hydrogen as a light element component of Earth's core (*6, 13*).

Previous diamond-cell experiments indicated that exposure to hydrogen at high pressures results in large deformation and embrittlement of steel gaskets used to contain the samples. To characterize the pressure-induced chemical reactivity of hydrogen and pure iron, a series of experiments was performed in which iron samples were loaded with hydrogen (initial molar ratio of iron:hydrogen ranged from 1:16 to 3:1) into a Mao-Bell diamond-anvil cell (*14*). The iron samples were typically located at the bottom of the sample chamber, surrounded by fluid (<5.5 GPa) or solid (>5.5 GPa) hydrogen at 298 K (*15*). In each experiment, the volume of the sample abruptly increased as the pressure was raised above 3.5 GPa (Fig. 1). This change was accompanied by a sudden streaming of the fluid hydrogen surrounding the metal and a textural change in the sample from smooth and lustrous to granular. These changes illustrate the loss of integrity of the metallic sample by hydrogen attack. To our knowledge this is the first report of the direct optical observation of a pressure-induced expansion.

To examine whether the observed expansion and morphological change are associated with a chemical reaction in the bulk sample, we performed a series of x-ray diffraction measurements as a function of pressure. The first experiments were done with a 50-mm-radius Debye-Scherrer camera and molybdenum radiation from a rotating anode x-ray source. Below 3.5 GPa, only diffraction lines from the body-centered cubic (bcc) phase of iron, which is stable in the absence of hydrogen to 13.1 GPa (*16*), were present. Once the pressure was raised and the iron had expanded, we observed new lines accompanying those of bcc iron. These new lines were due to iron hydride (*17*), but many were too closely spaced to be resolved.

To obtain higher resolution, we measured the diffraction pattern using synchrotron radiation techniques. Energy dispersive diffraction with high-energy synchrotron radiation has been found to provide excellent resolution if low diffraction angles and high-energy (>35 keV) radiation are used (*18*).

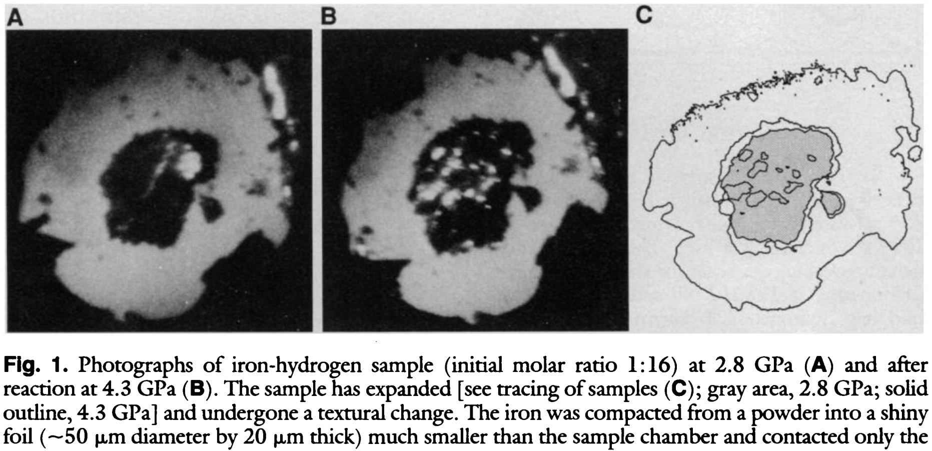

Fig. 1. Photographs of iron-hydrogen sample (initial molar ratio 1:16) at 2.8 GPa (**A**) and after reaction at 4.3 GPa (**B**). The sample has expanded [see tracing of samples (**C**); gray area, 2.8 GPa; solid outline, 4.3 GPa] and undergone a textural change. The iron was compacted from a powder into a shiny foil (~50 μm diameter by 20 μm thick) much smaller than the sample chamber and contacted only the culet of the bottom diamond. As fluid hydrogen filled the chamber, the pressure conditions were hydrostatic. Reaction with the walls of the iron gasket is likely to have occurred (see text), but a large excess of hydrogen remains.

Geophysical Laboratory and Center for High Pressure Research, Carnegie Institution of Washington, 5251 Broad Branch Road, N.W., Washington, DC 20015.

The iron hydride diffraction lines in energy-dispersive diffraction patterns, collected using a high-energy synchrotron source, were better resolved (Fig. 2). Similar results were obtained using film methods (*19*) and a monochromatic synchrotron source. The lattice parameter of bcc iron at 3.19 GPa (Fig. 2) agrees within 0.08% with the study of Mao *et al.* (*16*), showing that the bulk solubility of hydrogen in iron at this pressure is low. By 3.79 GPa, a multiplet near $d \sim 2.2$ Å and four more diffraction lines have appeared in addition to those of bcc iron. After the formation of iron hydride, the bcc diffraction lines gradually decreased in intensity with increasing pressure and disappeared between 9.45 and 14.7 GPa. Except for a shift in position and line width, no significant change in the iron hydride diffraction pattern was observed to the highest pressure measured, 62 GPa. The diffraction data also show that formation of iron hydride is reversible: the reaction can be driven rapidly toward iron or iron hydride by cycling the pressure.

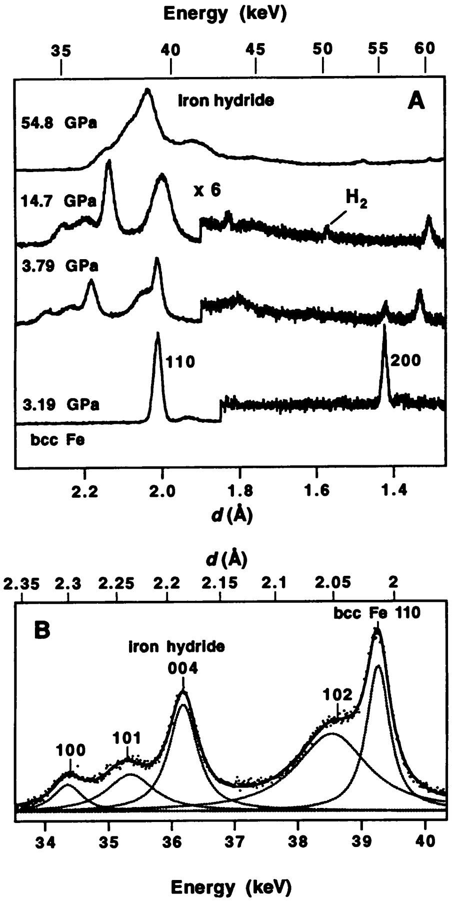

Fig. 2. (**A**) Energy dispersive x-ray diffraction patterns at different pressures. A diffraction angle of 9° was used except for measurements above 40 GPa for which 15° was used. The top axis shows the reciprocal energy scale for the measurements performed at 9°. The 101 diffraction line from the solid hcp hydrogen (*23*) surrounding the iron hydride sample was observed at 14.7 GPa, which illustrates the extremely high sensitivity of the synchrotron diffraction technique. (**B**) Expansion of the multiplet near $d \sim 2.1$ Å at a pressure of 3.79 GPa. The peaks were fit to a pseudo-Voight line profile and indexed on the basis of the dhcp structure. Measurements were performed at line X17C at the National Synchrotron Light Source.

The diffraction lines can be fit (*20*) (Table 1) to the double hexagonal close-packed (dhcp) structure (Fig. 3) with measured intensities in qualitative agreement with those calculated for this structure (*21*). The stacking sequence of closest packed layers for dhcp follows the pattern ABAC, with a *c* axis (~8.7 Å for iron hydride) twice the length of the hcp stacking AB, where A, B, and C represent the three possible orientations of the layers. The dhcp structure contains two different crystallographic iron sites owing to the presence of both B- and C-type layers (Fig. 3). It provides a basis for interpretation of high-pressure Mössbauer spectra, which suggest the presence of two iron sites (*22*). The results are also consistent with the structure determined by Antonov *et al.* (*9*) for iron hydride synthesized at high pressure and quenched to a metastable form at liquid nitrogen temperatures.

The pressure-volume relations (Fig. 4) determined from the diffraction data illustrate the large expansion in molar volume caused by the hydrogen. The expansion in cell volume upon reaction at 3.5 GPa, for example, is approximately 1.8 $Å^3$ per hydrogen. This is much larger than that required by packing considerations and illustrates the large changes in the bonding induced by the hydrogens (*3*). The data provide a determination of the stoichiometry, which has been a difficult problem in metal hydride chemistry. For almost all transition metal hydrides at ambient pressure, the increase in cell volume is approximately 2.9 $Å^3$ per hydrogen (*3*). By this analysis, with a difference in the fitted zero pressure volumes of iron hydride [55.6 (± 0.5) $Å^3$] and hcp iron (2 × 22.35 $Å^3$) of 10.9 $Å^3$, a composition of $FeH_{0.94}$ is obtained. Antonov *et al.* (*9*) estimated the stoichiometry to be $FeH_{0.86}$ from measurements of hydrogen evolved during decomposition of pressure-quenched samples. The discrepancy in stoichiometry is likely attributable to failure to trap all of the hydrogen in quenching. Based on the behavior of related compounds (*3*), we propose that the hydrogens in iron hydride occupy the octahedral interstices of the dhcp structure. If all these sites are filled, the stoichiometry would be 1:1, in good agreement with that determined from the cell-volume expansion.

To determine if the stoichiometry can vary, energy-dispersive diffraction data were collected to 32 GPa on an iron-hydrogen sample that contained sufficient iron (approximately 3:1 molar ratio) to insure that an excess remained after reaction. The diffraction patterns showed that both iron and iron hydride coexisted above 3.5 GPa. The cell volumes determined for iron hydride in this sample agree within the estimated error

Table 1. Observed interplanar distances, intensities, and peak widths for iron hydride at 3.79 GPa. The calculated *d*'s and intensities for a dhcp structure are shown as well. No correction was made for the decrease in incident beam intensity and scattering power with increasing energy (>20 keV) of the synchrotron beam. Therefore, the measured peaks at the highest energies are considerably weaker than the calculated values.

d_{obs} (Å)	d_{calc} (Å)	Δd (Å)	*hkl*	I_{obs}	I_{calc}	fwhm (keV)
2.299	2.309	−0.010	100	14	8	0.54
2.242	2.232	0.010	101	32	43	0.90
2.184	2.184	0.000	004	56	36	0.55
2.050	2.041	0.009	102	100	100	1.35
2.013			bcc Fe 110	69		0.44
1.809	1.809	0.000	103	4	23	1.18
	1.587		104		5	
1.422			bcc Fe 200	3		0.56
	1.393		105		10	
1.333	1.333	0.000	110	8	22	0.70
	1.232		106		18	
1.160	1.154	0.006	200	vw	1	1.1
	1.145		201		5	
1.141	1.138	0.003	114	vw	24	0.51

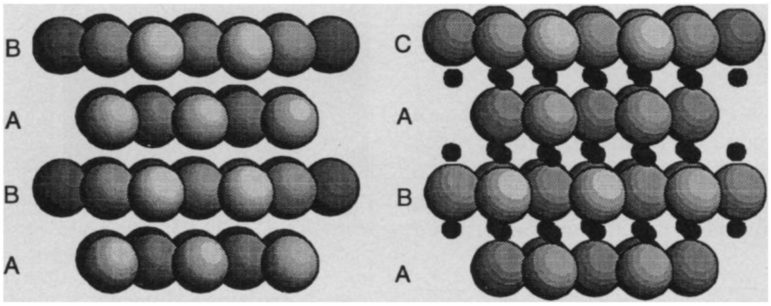

Fig. 3. (**Left**) Hexagonal close-packed (hcp) crystal structure of iron and (**right**) double hexagonal close-packed (dhcp) crystal structure of iron hydride with interstitial hydrogens at octahedral sites.

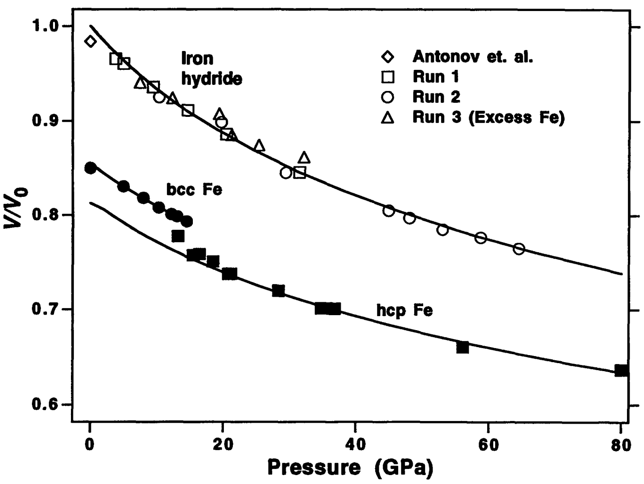

Fig. 4. Pressure-volume relations for bcc iron, hcp iron, and iron hydride in the presence of both excess hydrogen (runs 1 and 2) and excess iron (run 3). The equation of state of Vinet (*32*) was used to fit the pressure-volume curves [iron hydride: V_0 = 55.6 ± 0.5 Å^3, K_0 = 121 ± 19 GPa, K_0' = 5.31 ± 0.9; hcp iron: V_0 = 22.35 ± 0.03 Å^3, K_0 = 160.2 ± 2.1 GPa, K_0' = 5.82 ± 0.08 (*23*)]. The unit-cell volumes are normalized to the zero-pressure volume (V_0) of iron hydride. The volume determined by Antonov *et al.* for quenched iron hydride is also shown (*9*); it is slightly less than V_0 due to contraction of the cell volume at 90 K. Iron hydride has four iron atoms per unit cell, whereas bcc and hcp iron have only two iron atoms per unit cell. The errors are estimated to be 3% in pressure and 0.3% in volume (T = 298 K).

of the measurements with those of the sample containing excess hydrogen (Fig. 4). Since the cell volume is a sensitive indicator of the amount of hydrogen incorporated (*3*), we conclude that iron hydride must be of fixed stoichiometry over this pressure range.

The equation of state of a material is important for assessing its stability and structure-property relations at high pressure. Iron hydride, with a bulk modulus of 121 (± 19) GPa, is more compressible than hcp iron [160 (± 2) GPa]. At 3.5 GPa the volume of iron hydride is 8.54 cm^3 per mole (51%) less than that of an equimolar iron-hydrogen mixture (*16, 23*). At 60 GPa the measured difference is 5.46 cm^3 per mole (*24*); by extrapolation of the equations of state of the products and reactants, we estimate that iron hydride should be stable to pressures in excess of 100 GPa. Many transition metal hydrides have "incompressible" interstitial hydrogens such that the difference in cell volume between hydride and metal is only weakly dependent on pressure (*3*). In contrast, we find that the difference in cell volume between iron hydride and hcp iron decreases by 35% from 3.5 to 60 GPa (10.4 to 6.8 Å^3). We infer that this decrease in volume must be associated with changes in the electronic properties of the hydrogens. Fukai (*3*) has correlated the effect of pressure on the volume per hydrogen in metal hydrides with that expected for metallic atomic hydrogen at very high densities. Our results give hydrogen volumes that are significantly smaller than these estimates (1.7 Å^3 per hydrogen at 60 GPa).

At low pressures (>0.1 GPa) the iron-hydrogen phase diagram has been thoroughly studied and the hydrogen concentration in iron does not exceed 0.05 atomic percent (*25*). Though the bulk solubility remains low below 3.5 GPa, iron and ferrous alloys can be significantly weakened and embrittled at these pressures (*26*). In several experiments, for example, the stainless steel gaskets, 1-inch-diameter disks that were 250 μm thick and subjected to a pressure of 0.2 GPa of hydrogen during loading, were embrittled and cracked into large pieces after removal from the diamond cell. In high-pressure diamond-cell experiments with hydrogen, the steel surrounding the gasket hole has greater tendency to flow and the gasket holes tend to deform severely, particularly at pressures above 60 GPa (*11*). After unloading, the steel surrounding the gasket hole was severely disrupted and tended to flake into small pieces. This is likely a result of formation of iron hydride at the sample-gasket interface. Formation of iron hydride will expand, disrupt, and weaken the metal, which then falls apart upon contracting after unloading. Experiments with rhenium as a gasket material result in smaller hole deformation (higher sample stability) in ultrahigh pressure experiments on hydrogen samples (*27*). Rhenium hydride has been synthesized (*28*), but detailed information about its formation and properties at high pressure is not available. Characterization of such pressure-induced reactions involving hydrogen will be important for containment of hydrogen at still higher pressures in the diamond cell.

Finally, the high-pressure stability and equation of state measurements of iron hydride have implications for the composition of Earth's core. Seismological measurements document that Earth's core is less dense than expected for hcp iron under core conditions by approximately 10% (*29*). Iron hydride has been proposed as a component to account for the decreased density (*6, 13*), but no measurements of its high-pressure stability and pressure-density relations were available. Our measured equation of state shows that at pressures of the inner core/outer core boundary (330 GPa) and 25°C the density of iron hydride is 12.5 g cm^{-3}, which compares with a density of 12.2 g cm^{-3} obtained from seismology (*29*). If we assume core temperatures of 4000 to 6000 K and values for the thermal expansion coefficient assumed for iron under these conditions (8 × 10^{-6} to 16 × 10^{-6} K^{-1}) (*30*), we find that a mole fraction of iron hydride in the core ranging from 40 to 95% can be consistent with the measured core density (*31*). The effect of other light elements and the amount of hydrogen retained in Earth following accretion needs to be examined (*29*). Our results show that a large hydrogen component of the core is compatible with current seismological data.

REFERENCES AND NOTES

1. For a review, see R. J. Hemley, H. K. Mao, M. Hanfland, in *Molecular Systems Under High Pressure*, R. Pucci and G. Piccitto, Eds. (Elsevier, Amsterdam, 1991), pp. 223–243.
2. *Z. Physik. Chem.* **163**, 420 (1989).
3. Y. Fukai, *J. Less Common Metals*, in press; B. Baranowski, in *Molecular Systems Under High Pressure*, R. Pucci and G. Piccitto, Eds. (Elsevier, Amsterdam, 1991), pp. 139–156.
4. G. Alefeld and J. Völkl, Eds., *Hydrogen in Metals I* (Springer-Verlag, New York, 1978); N. W. Ashcroft, *Phys. Rev. Lett.* **21**, 1748 (1968). The hydrogen vibrations of metallic hydrogen and hydrides can exhibit large amplitudes, considerable anharmonicity, and strong coupling to the electrons. This has stimulated interest in the dynamical properties of these systems, especially possible high-temperature superconductivity.
5. R. A. Oriani, J. P. Hirth, M. Smialowski, Eds., *Hydrogen Degradation of Ferrous Alloys* (Noyes, Park Ridge, NJ, 1985).
6. See, for example, Y. Fukai and T. Suzuki, *J. Geophys. Res. B* **91**, 9222 (1986); J. A. Jacobs, *The Earth's Core* (Academic Press, London, ed. 2, 1987), pp. 321–336.
7. N. N. Greenwood and A. Earnshaw, *Chemistry of the Elements* (Pergamon, Oxford, 1981), pp. 71–72; Transition metal hydride stability decreases from scandium toward the right of the periodic table, until the group of metals to the right of chromium, which do not have stable hydrides under ambient conditions. Palladium hydride is a notable exception to this "hydrogen gap."
8. V. E. Antonov, I. T. Belash, E. G. Degtyareva, E. G. Ponyatovskii, I. Shiraev, *Sov. Phys. Dokl.* **25**, 490 (1980); V. E. Antonov, I. T. Belash, E. G. Ponyatovskii, *Script. Met.* **16**, 203 (1982).
9. V. E. Antonov *et al.*, *Int. J. Hydrogen Energy* **14**, 371 (1989).
10. A. Jayaraman, *Rev. Mod. Phys.* **55**, 65 (1983); *Rev. Sci. Instrum.* **57**, 1013 (1986); R. Jeanloz, *Annu. Rev. Phys. Chem.* **40**, 237 (1989); H. K. Mao, in *Simple Molecular Systems at Very High Densities*, A. Polian, P. Loubeyre, N. Bocarra, Eds. (Plenum, New York, 1989), pp. 221–236.
11. R. J. Hemley and H. K. Mao, *Phys. Rev. Lett.* **61**, 857 (1988); H. K. Mao and R. J. Hemley, *Science* **244**, 1462 (1989).
12. R. Wiswall, in *Hydrogen in Metals II*, G. Alefeld and J. Völkl, Eds. (Springer, Berlin, 1978), pp. 201–238.
13. W. Kuhn and A. Rittman, *Geol. Rundschau* **32**, 215

(1941); R. Kronig, J. De Boer, J. Korringa, *Physica* **XII**, 245 (1946); D. J. Stevenson, *Nature* **268**, 130 (1977); Y. Fukai, *ibid.* **308**, 174 (1984).

14. Hydrogen was loaded into the diamond cell with T301 stainless steel gaskets at a pressure of 0.2 GPa [A. P. Jephcoat, H. K. Mao, P. M. Bell, in *Hydrothermal Experimental Techniques*, G. C. Ulmer and H. L. Barnes, Eds. (Wiley, New York, 1987), p. 469]. Pressure measurements were performed using ruby fluorescence; the R_1-R_2 splitting was well resolved up to 32 GPa [H. K. Mao, J. Xu, P. M. Bell, *J. Geophys. Res. B* **91**, 4673 (1986)].
15. H. K. Mao and P. M. Bell, *Science* **203**, 1004 (1979).
16. H. K. Mao, W. A. Bassett, T. Takahashi, *J. Appl. Phys.* **38**, 272 (1967).
17. Antonov *et al.* obtained indirect evidence for a reaction between iron and hydrogen at 3.5 GPa from electrical resistivity measurements (*8*).
18. J. V. Badding, H. K. Mao, R. J. Hemley, *Solid State Comm.* **77**, 801 (1990).
19. C. Meade and R. Jeanloz, *Rev. Sci. Instrum.* **61**, 2571 (1990).
20. A. D. Mighell, C. R. Hubbard, J. K. Stalick, M. A. Holomany, *BookNBS*AIDS83: A Manual Describing the Data Format Used in NBS*AIDS83* (JCPDS-International Centre for Diffraction Data, Swarthmore, PA, 1983); the figure of merit for the fit ranged from 13 to 23. Peak positions were determined by a fit to a pseudo-Voight line profile [L. W. Finger, in *Reviews in Mineralogy*, D. L. Bish and J. E. Post, Eds. (Mineralogical Society of America, Washington, DC, 1989), vol. 20, p. 309].
21. The accuracy of intensity measurements in the diamond cell can be limited by preferred orientation, which is often observed because the small sample size can make it difficult to sample a truly random set of diffraction planes [H. K. Mao *et al.*, *Phys. Rev. Lett.* **64**, 1749 (1990)].
22. I. Choe, R. Ingalls, J. M. Brown, Y. Sato-Sorensen, R. Mills, *Phys. Rev. B*, in press.
23. H. K. Mao *et al.*, *Science* **239**, 1131 (1988).
24. H. K. Mao, Y. Wu, L. C. Chen, J. F. Shu, A. P. Jephcoat, *J. Geophys. Res. B* **95**, 21737 (1990).
25. F. E. Fujita, in *Hydrogen Degradation of Ferrous Alloys*, R A. Oriani, J. P. Hirth, M. Smialowski, Eds. (Noyes, Park Ridge, NJ, 1985), pp. 1–14.
26. Although pressures of 0.2 GPa are insufficient to form bulk hydride, hydrogen can become trapped in cracks and voids where its fugacity can be increased by high local stresses, which will enhance its concentration locally in the surrounding steel [C. A. Wert, in *Hydrogen in Metals II*, G. Alefeld and J. Völkl, Eds. (Springer-Verlag, New York, 1978), pp. 305–328; H. P. van Leeuwen, in *Hydrogen Degradation of Ferrous Alloys*, R. A. Oriani, J. P. Hirth, M. Smialowski, Eds. (Noyes, Park Ridge, NJ, 1985), pp. 17–23]. It is difficult to directly probe the properties of metals near cracks and voids and the mechanism of embrittlement is poorly understood; bulk high pressure measurements such as those presented here can be used to determine the properties of ferrous hydrides or ferrous metals with high levels of hydrogen doping and aid our understanding of embrittlement.
27. R. J. Hemley and H. K. Mao, *Science* **249**, 391 (1990).
28. V. E. Antonov *et al.*, *Dokl. Akad. Nauk SSSR* **269**, 617 (1983); E. G. Ponyatovskii and V. E. Antonov, in *Problems in Solid-State Physics*, A. M. Prokhorov and A. S. Prokhorov, Eds. (MIR, Moscow, 1984), p. 109.
29. R. Jeanloz, *Annu. Rev. Earth Planet Sci.* **18**, 357 (1990).
30. A. Jephcoat and P. Olson, *Nature* **325**, 332 (1987).
31. J. V. Badding, H. K. Mao, R. J. Hemley, in preparation.
32. P. Vinet, J. Ferrante, J. Smith, J. H. Rose, *J. Phys. C* **19**, L467 (1986).
33. We thank C. Meade, L. W. Finger, R. E. Cohen, R. Jeanloz, and J. M. Brown for valuable discussions and comments on the manuscript. This work was supported by the National Science Foundation under grants EAR-8904080, EAR-8720320, and DMR-8912226 and the Carnegie Institution of Washington.

9 May 1991; accepted 12 June 1991

Commensurability and Mobility in Two-Dimensional Molecular Patterns on Graphite

JÜRGEN P. RABE* AND STEFAN BUCHHOLZ

Two-dimensional molecular patterns were obtained by the adsorption of long-chain alkanes, alcohols, fatty acids, and a dialkylbenzene from organic solutions onto the basal plane of graphite. In situ scanning tunneling microscopy (STM) studies revealed that these molecules organize in lamellae with the extended alkyl chains oriented parallel to a lattice axis within the basal plane of graphite. The planes of the carbon skeletons, however, can be oriented either predominantly perpendicular to or predominantly parallel with the substrate surface, causing the lamellar lattice to be either in or near registry with the substrate (alkanes and alcohols) or not in registry (fatty acids and dialkylbenzenes). In the case of the alcohols and the dialkylbenzene the molecular axes are tilted by +30° or −30° with respect to an axis normal to the lamella boundaries, giving rise to molecularly well-defined domain boundaries. Fast STM image recording allowed the spontaneous switch between the two tilt angles to be observed in the alcohol monolayers on a time scale of a few milliseconds.

ORGANIC MONOLAYERS OF MOLECULAR thickness play an important role in many interfacial phenomena, including wetting, lubrication and adhesion, and molecular and biological recognition. In addition, well-defined monolayers on inert supports are suitable model systems for the investigation of two-dimensional (2-D) phenomena. Because of a lack of true crystallinity in two dimensions, their in-plane structure remains, however, a challenge for both theory and experiment. For rare gas atoms under ultrahigh vacuum and at low temperatures, scattering methods have been successfully used to elucidate their typical 2-D behavior (*1*). Langmuir-Blodgett layers have also been investigated using, for example, electron scattering (*2*), x-ray scattering (*3, 4*), and Raman scattering methods (*5*), both in vacuum or under ambient conditions. With the help of STM (*6, 7*) it has become possible to directly observe structure and dynamics at solid-fluid interfaces in situ on the relevant length scales, that is, from the atomic scale to the micrometer scale and larger. In particular, STM images provide detailed information on the commensurability between molecular adsorbate and substrate lattices. A related issue, the mobility within the monolayer, can be observed by STM on a time scale of a few milliseconds (*7*). We demonstrate the cooperative reorientation in nanometer-size domains in a 2-D polycrystal. Information of this kind may improve our understanding of the mechanisms underlying various interfacial processes, including boundary lubrication, and may help in the development of theoretical models for molecular dynamics simulations of molecular monolayers. Finally, our increasing ability to characterize these systems will be important for efforts to generate a 2-D molecular patterns (*8*) on the submicrometer scale approaching nanometer dimensions. The latter may eventually prove useful for information storage.

Adsorption isotherms and enthalpies of adsorption (*9–11*) indicate that long-chain alkanes, alcohols, fatty acids, and alkylbenzenes adsorb as monomolecular layers from nonpolar organic solvents to the basal plane of graphite. However, there has been debate about whether the alkane adsorption is driven by the registry between the carbon lattices of adsorbate and substrate (*9*) or by a 2-D crystallization of the adsorbate on a flat substrate, independent of the substrate lattice (*10*). We present a detailed analysis of the order in monolayers of simple long-chain alkyl derivatives physisorbed at room temperature at the interface between the basal plane of graphite and an organic solution. It shows, in particular, the difference in registry in the directions parallel with and perpendicular to the alkane chains.

In order to observe nonconducting molecular adsorbates by STM, it is necessary that the adsorbate modifies the tunneling current sufficiently. This modification may be caused either by a change of the tunneling barrier (*12–15*) or by a change in the density of states within substrate or tip, due to their electronic interaction with the adsorbate (*16, 17*). In any case the image contrast depends on the tunneling bias. If under certain bias conditions the adsorbate modifies the tunneling current strongly, the image will be dominated by the adsorbate; if the modification is weak, the image will be dominated by the substrate. Particularly interesting for structure analysis is the case in which the image contains information about both substrate and adsorbate structure si-

---

Max-Planck-Institut für Polymerforschung, Postfach 3148, D-6500 Mainz, Germany.

*To whom correspondence should be addressed.